Variable Resonant Frequency Crystal Systems

WILLIAM J. FRY, RUTH BAUMANN FRY, AND WAYNE HALL
University of Illinois, Urbana, Illinois

(Received June 13, 1950)

A general analysis of variable resonant frequency crystal systems which utilize liquid media as backing is presented. Formulas are obtained for evaluating the effect of different geometries of backing on the resonant frequencies of the system. The various loss factors associated with such a system are related to the measurable quantity, the quality factor.

The observed operating characteristics of a variable resonant system which covers a two-to-one frequency band (40 kc to 80 kc) are presented. The results of an experimental comparison of such a system with fixed resonant frequency systems for generation of ultrasound in liquid media are given. The theory is used to correlate the experimental observations.

I. INTRODUCTION

THE study of fixed resonant frequency piezoelectric crystal systems has received considerable attention in the literature.[1] At the present time, systems employing piezoelectric materials operating at resonance are used in electrical oscillator control, filters, underwater sound locating devices, and high power ultrasonic generators.

In this paper, we are interested in variable resonant frequency systems. The characteristics obtainable for such systems will determine their range of application. The application of immediate interest to us is the problem of producing high intensity ultrasound over a continuous frequency range in liquid media. The present paper is concerned with the electrical and acoustic characteristics of units for operation at frequencies above the audible range but less than about 200 kc.

Theoretical results derived are used to correlate the experimental measurements. We are interested in particular in a detailed analysis of the acoustical properties of the backing material which is utilized to shift the resonant frequency of the system over a continuous range of frequencies.

Since most of our experimental work has been with backing systems of the order of several wavelengths or less, in maximum dimensions, the development of the theory in this paper will be especially suited to that case. The graphical presentation of pertinent formulas is useful for the design of a variety of variable resonant frequency crystal systems. Other investigators have reported research on variable resonant frequency crystal systems. A paper by Fox and Rock on quartz plates with coupled liquid columns presents experimental data obtained for the equivalent electrical constants of such systems.[2] The results are correlated on the basis of a lumped circuit theory for the motional part of the electrical input impedance of the crystal system.[3–5]

From the paper of Fox and Rock, it appears that the reduction of the losses of vibrational energy was not a primary concern of these investigators. In this paper, we will be interested in analyzing the sources of loss of vibrational energy in variable resonant frequency crystal systems.

Since we wish to obtain a system to operate at resonance over a relatively wide frequency range (a frequency ratio of two to one or more), it is convenient to use a liquid as the backing material. In order to minimize loss, it is desirable to choose a liquid of low absorption coefficient. The density and characteristic acoustic impedance of the liquid are factors in determining the resonant frequencies of the system as a function of the dimensions of the backing material.

The use of a liquid as backing requires a container for support which will decouple the liquid from the supporting structure. Furthermore, the rate of acoustical energy absorption at the interfaces must be relatively small. A high reflection coefficient combined with mechanical stability is necessary.

In order to realize an efficient system over a wide frequency range, it is essential to have tight coupling between the crystal and the backing liquid. This involves either the wettability of the crystal by the liquid directly, or, the use of suitable coupling materials interposed between the crystal and the backing liquid.

Let us consider a crystal system of the type illustrated schematically in Fig. 1. The diagram exhibits a crystal unit consisting of one or more crystals, cut to vibrate in either longitudinal or thickness mode, mounted flush in one wall of an enclosure. This enclosure serves as a container for the liquid which is used as a backing material for the crystal unit. The container confines the liquid so that there is no free surface. A movable piston opposite the wall in which the crystal unit is mounted enables the volume of liquid to be continuously varied. A coupling material is shown interposed between the crystal and the liquid. The end of the unit opposite the container can be coupled to the system in which acoustic radiation is desired.

Quantities which are of interest in the present study of variable resonant frequency crystal systems are:

[1] For extensive bibliographies see W. G. Cady, *Piezoelectricity* (McGraw-Hill Book Company, Inc., New York, 1946) and L. Bergmann, *Ultrasonics* (John Wiley and Sons, Inc., New York, 1946).
[2] F. E. Fox and G. D. Rock, Proc. IRE **30**, 29 (1942).
[3] J. C. Hubbard, Phys. Rev. **38**, 1011 (1931).
[4] J. C. Hubbard, Phys. Rev. **41**, 523 (1932).
[5] F. E. Fox, Phys. Rev. **52**, 973 (1937).

resonant frequencies, electrical input impedance at resonance with the unit not radiating, quality factor (defined below) under the same conditions, and transmitting response with the unit radiating. All of these quantities, with the possible exception of the quality factor, can be readily determined experimentally. Accurate determination of this quantity requires that the resonant frequencies of the crystal system be fairly well separated. When this is not the case, a measurement of the Q at resonance is more convenient. From a theoretical point of view, we shall be most interested in the resonant frequency characteristics and the quality factor, defined as the ratio of the antiresonant impedance to the resonant impedance. If the quality factor of the system is high under nonradiating conditions, it will operate efficiently as a source of acoustic energy.

Initially, we will be concerned with an analysis of systems which contain no losses. This part of the theory will enable us to determine the resonant frequencies of the system as a function of the geometrical arrangement and relative dimensions of the crystal unit and the backing. A one-dimensional theory for the backing fluid is inadequate in the theoretical development. However, a one-dimensional theory for the crystal is employed in the analysis. This appears to be sufficiently accurate for our present purposes, particularly, if we determine an "effective sound velocity" for the crystal from resonant frequency data on free crystals as explained in detail below. It is assumed that the face of the crystal which excites the backing liquid through the coupling material vibrates as a rigid piston.

The theoretical development for the no-loss system is carried out for both the case of a rigid wall (zero normal velocity) in which the crystal unit is mounted and for a pressure-release wall (pressure zero) in which the crystal is mounted. All other walls are taken as pressure-release for both cases. In the experimental work, pressure-release walls have been utilized throughout. However, it is desirable to compare the input impedance relations for both cases in order to determine ranges of values of the parameters over which the rigid end case could be used to approximate closely the pressure-release end case. This is desirable, since the amount of numerical calculation required for applying the resultant formulas for the pressure-release case is greatly in excess of the amount required for applying the formulas for the rigid end case.

Various factors, other than radiation, contribute toward the loss of vibrational energy in a crystal system. Reference to Fig. 1 will indicate the possibilities. We list them as follows: (1) internal losses in the crystal; (2) internal losses in the backing medium; (3) loss at the crystal coupling material interface; (4) loss at the interface of the coupling material and the backing liquid; (5) loss at the bond between the crystal unit and the supporting wall and the internal bonds if the unit is a multiple crystal assembly; and (6) loss at the liquid decoupling material interface.

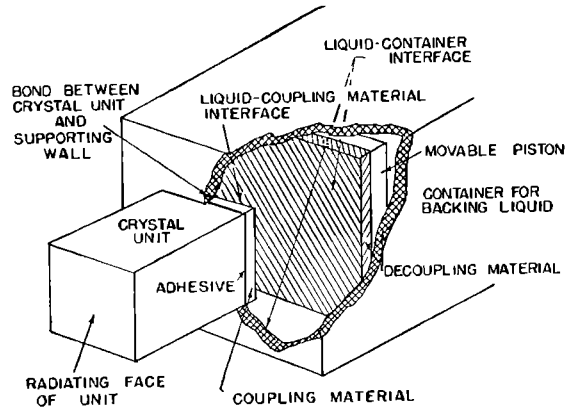

FIG. 1. Diagram of a variable resonant frequency unit.

All of the various loss factors which contribute appreciably toward the total loss of the system are combined to yield the resistive component of the input acoustic impedance of the backing materials at the crystal coupling material interface. The quality factor for the nonradiating system then follows from the relation expressing this quantity as a function of the terminating impedance of the crystal.

II. THEORY

1. Lossless Systems

As indicated above, we are concerned first with an analysis of the acoustics of the backing material under the assumption that there is no loss of acoustic energy. This treatment utilizes a mode method of analysis.[6,7]

Impedance Functions

A piezoelectric crystal looks into a medium from one wall of a rectangular container. The crystal face is centered symmetrically in the plane of the supporting wall (Fig. 2a).

The planes of the system specified with respect to rectangular coordinates are as follows:

$$\begin{aligned} x&=0, \quad x=L_1; \\ y&=0, \quad y=L_2; \\ z&=0, \quad z=L_3. \end{aligned}$$

The boundaries of the crystal mounted in the plane $x=0$ are

$$\begin{aligned} y&=\tfrac{1}{2}L_2-s, \quad y=\tfrac{1}{2}L_2+s; \\ z&=\tfrac{1}{2}L_3-r, \quad z=\tfrac{1}{2}L_3+r, \end{aligned}$$

as indicated in Fig. 2b.

An acoustical disturbance in the medium will be expressed in terms of the pressure. When the amplitude of the vibration is small, this function satisfies the

[6] See for example, P. M. Morse, *Vibration and Sound* (McGraw-Hill Book Company, Inc., New York, 1948).
[7] W. J. Jacobi, J. Acoust. Soc. Am. 21, 120 (1949).

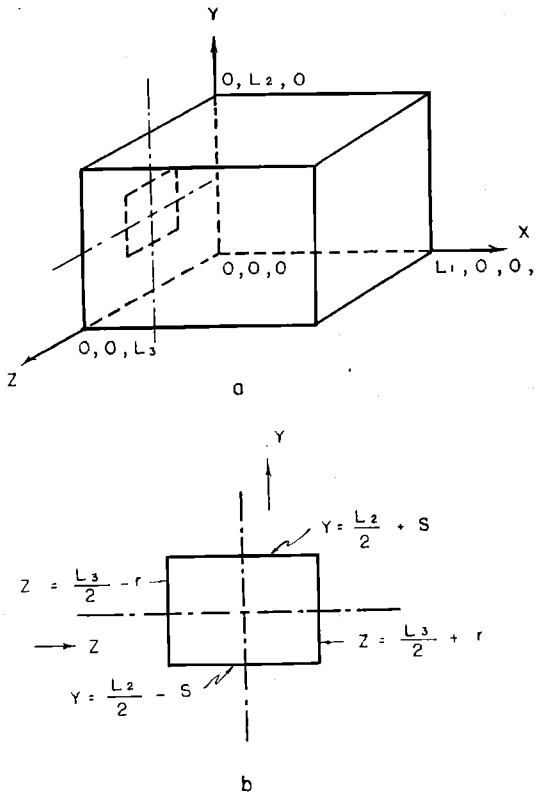

FIG. 2. (a) Support for backing liquid placed in a coordinate system. (b) Coordinate position of crystal face at $x=0$.

equation

$$\nabla^2 p=(1/V^2)\partial^2 p/\partial t^2.$$

For sinusoidal time variation, $p=Pe^{j\omega t}$ and, therefore

$$\nabla^2 P+k^2 P=0, \tag{1}$$

where $k=\omega/V$.

Case 1.—We will consider first a disturbance which satisfies the following boundary conditions:

(1) the five free walls are pressure-release surfaces ($P=0$);

(2) the normal particle velocity over the wall in which the crystal is mounted is zero;

(3) the x component of the particle velocity for the crystal face looking into the medium is constant $[u_x=(j/\omega\rho)(\partial P/\partial x)_{x=0}=C']$.

Applying the method of separation of variables to Eq. (1) functions of the form:

(a) $h(z)=a\sin(Rz+b)$
(b) $g(y)=c\sin(Sy+d)$
(c) $f(x)=e\sin[(k^2-R^2-S^2)^{\frac{1}{2}}x+f]$ are obtained,

where $P=f(x)g(y)h(z)$, and R and S are separation constants.

Inserting the boundary conditions $P=0$, or $h(z)=0$, when $z=0$, $z=L_3$; $P=0$, or $g(y)=0$, when $y=0$, $y=L_2$ in solutions (a) and (b), respectively, we conclude

(a′) $h(z)=a\sin(n\pi z/L_3)$ $n=1, 2, 3, \cdots$
(b′) $g(y)=c\sin(m\pi y/L_2)$ $m=1, 2, 3, \cdots$.

When $x=L_1$, $P=0$, and $f(x)=0$, so that expression (c) becomes

(c′) $f(x)=e\sin\{[k^2-(n\pi/L_3)^2-(m\pi/L_2)^2]^{\frac{1}{2}}(x-L_1)\}$.

In order to obtain an expression which will satisfy the boundary conditions at $x=0$, we form the sum

$$P=\sum_{nm} A_{nm}\sin\frac{n\pi z}{L_3}\sin\frac{m\pi y}{L_2}\sin\left\{\left[k^2-\left(\frac{n\pi}{L_3}\right)^2-\left(\frac{m\pi}{L_2}\right)^2\right]^{\frac{1}{2}}(x-L_1)\right\}. \tag{2}$$

For the purpose of evaluating the coefficients A_{nm}, we note that the particle velocity in the x direction is constant at the crystal face and that the particle velocity over the remainder of the face is zero. The coefficients A_{nm} are then given by the integral relation

$$A_{nm}\left[k^2-\left(\frac{n\pi}{L_3}\right)^2-\left(\frac{m\pi}{L_2}\right)^2\right]^{\frac{1}{2}}\cos\left\{-L_1\left[k^2-\left(\frac{n\pi}{L_3}\right)^2-\left(\frac{m\pi}{L_2}\right)^2\right]^{\frac{1}{2}}\right\}=\frac{4C}{L_2L_3}\int_{\frac{1}{2}L_2-s}^{\frac{1}{2}L_2+s}\int_{\frac{1}{2}L_3-r}^{\frac{1}{2}L_3+r}\sin\frac{n\pi z}{L_3}\sin\frac{m\pi y}{L_2}dzdy, \tag{3}$$

where $C=-j\omega\rho C'$. Thus the coefficients are evaluated as

$$A_{nm}=\frac{(-1)^{\frac{1}{2}(n+m-2)}2^4C\sin(n\pi r/L_3)\sin(m\pi s/L_2)}{\pi^2nm[k^2-(n\pi/L_3)^2-(m\pi/L_2)^2]^{\frac{1}{2}}\cos\{-L_1[k^2-(n\pi/L_3)^2-(m\pi/L_2)^2]^{\frac{1}{2}}\}} \tag{4}$$

for n and m odd integers only. Otherwise, $A_{nm}=0$.

The expression for the force on the medium at the crystal face is given by the relation

$$F=\int_{\frac{1}{2}L_2-s}^{\frac{1}{2}L_2+s}\int_{\frac{1}{2}L_3-r}^{\frac{1}{2}L_3+r}P dzdy.$$

The positive direction of the x axis is in the direction into the medium at this interface. Consequently,

$$F=\frac{4L_2L_3}{\pi^2}\sum_{nm}A_{nm}\sin\left\{-L_1\left[k^2-\left(\frac{n\pi}{L_3}\right)^2-\left(\frac{m\pi}{L_2}\right)^2\right]^{\frac{1}{2}}\right\}\frac{(-1)^{\frac{1}{2}(n+m-2)}}{nm}\sin\frac{n\pi r}{L_3}\sin\frac{m\pi s}{L_2}.$$

Substituting for A_{nm} from expression (4) and rearranging,

$$F=\frac{2^6CL_2L_3}{\pi^4}\sum_{nm}\frac{\tan\{-L_1[k^2-(n\pi/L_3)^2-(m\pi/L_2)^2]^{\frac{1}{2}}\}}{n^2m^2[k^2-(n\pi/L_3)^2-(m\pi/L_2)^2]^{\frac{1}{2}}}\sin^2(n\pi r/L_3)\sin^2(m\pi s/L_2), \tag{5}$$

summed over odd integral values of n and m only. Since $Z_m=F/C'$, the mechanical input impedance is

$$Z_m=j\omega\rho\frac{2^6}{\pi^5}L_1L_2L_3\sum_{nm}\frac{\tan\{\pi[(2L_1/\lambda)^2-(nL_1/L_3)^2-(mL_1/L_2)^2]^{\frac{1}{2}}\}}{n^2m^2[(2L_1/\lambda)^2-(nL_1/L_3)^2-(mL_1/L_2)^2]^{\frac{1}{2}}}\sin^2(n\pi r/L_3)\sin^2(m\pi s/L_2), \tag{6a}$$

where λ is the wavelength of the sound in the medium.

The average input acoustic impedance, Z_a, is given by the ratio of the mechanical impedance, Z_m, to the area, $4rs$; i.e.,

$$Z_a=\frac{Z_m}{4rs}=j\omega\rho\frac{2^4L_1L_2L_3}{\pi^5rs}\sum_{nm}\frac{\tan\{\pi[(2L_1/\lambda)^2-(nL_1/L_3)^2-(mL_1/L_2)^2]^{\frac{1}{2}}\}}{n^2m^2[(2L_1/\lambda)^2-(nL_1/L_3)^2-(mL_1/L_2)^2]^{\frac{1}{2}}}\sin^2(n\pi r/L_3)\sin^2(m\pi s/L_2). \tag{6b}$$

Introducing parameters defined by the ratios

$$L_1/\lambda=a_{1\lambda};\quad L_1/L_3=b_{13};\quad L_3/L_2=c_{32};$$

and the quantity E_{nm} defined by $E_{nm}=[4a_{1\lambda}^2-b_{13}^2(n^2+m^2c_{32}^2)]^{\frac{1}{2}}$ and substituting the value for ω in terms of the wavelength, $\omega=2\pi V/\lambda$, we obtain

$$\frac{Z_m}{j\rho V2^7/\pi^4}=L_2L_3a_{1\lambda}\sum_{nm}\frac{\tan\pi E_{nm}}{n^2m^2E_{nm}}\sin^2\frac{n\pi r}{L_3}\sin^2\frac{m\pi s}{L_2} \tag{7a}$$

and

$$\frac{Z_a}{j\rho V2^7/\pi^4}=\frac{L_2L_3a_{1\lambda}}{4rs}\sum_{nm}\frac{\tan\pi E_{nm}}{n^2m^2E_{nm}}\sin^2\frac{n\pi r}{L_3}\sin^2\frac{m\pi s}{L_2}. \tag{7b}$$

For the special case in which the cross-sectional area of the crystal is equal to that of the backing, that is, when $2r=L_3$ and $2s=L_2$, the above expressions reduce to

$$(Z_m/j\rho V)(\pi^4/2^7)=L_2L_3a_{1\lambda}\sum_{nm}\tan\pi E_{nm}/n^2m^2E_{nm} \tag{8a}$$

and

$$(Z_a/j\rho V)(\pi^4/2^7)=a_{1\lambda}\sum_{nm}\tan\pi E_{nm}/n^2m^2E_{nm}. \tag{8b}$$

It is of interest to observe at this point that as the cross-sectional dimensions become large, c_{32} remaining bounded and λ and L_1 being fixed, the expression (7b) reduces to the form

$$\frac{Z_a}{j\rho V2^7/\pi^4}=\frac{L_2L_3}{4rs}\frac{\tan2\pi a_{1\lambda}}{2}\sum_{nm}\frac{1}{n^2m^2}\sin^2\frac{n\pi r}{L_3}\sin^2\frac{m\pi s}{L_2}. \tag{9}$$

Upon evaluation of the summation[8] the expression further reduces to

$$Z_a=j\rho V\tan(\omega L_1/V), \tag{10}$$

which is the result obtained on the basis of a one-dimensional theory for the backing.

[8] E. T. Whittaker and G. N. Watson, *Modern Analysis* (Cambridge University Press, 1935), p. 167.

For the purpose of computing the resonant frequencies of crystal systems as a function of the dimensions of the liquid backing, expression (7b) is represented graphically. The graphs of Figs. 3, 4, 5, and 6 are plotted for a ratio of backing cross-section dimensions and crystal cross-section dimensions of 0.8; i.e., $c_{32}=0.8$ and $r/s=0.8$. The quantity $a_{1\lambda}$ is plotted as a function of b_{13} with the quantity $(Z_a/j\rho V)(\pi^4/2^7)$ as a parameter.

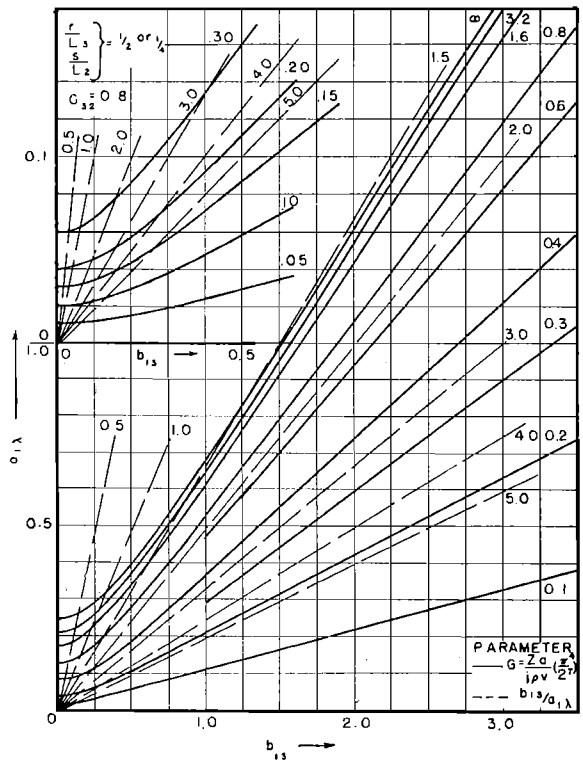

FIG. 3. Design curves, rigid wall at $x=0$.

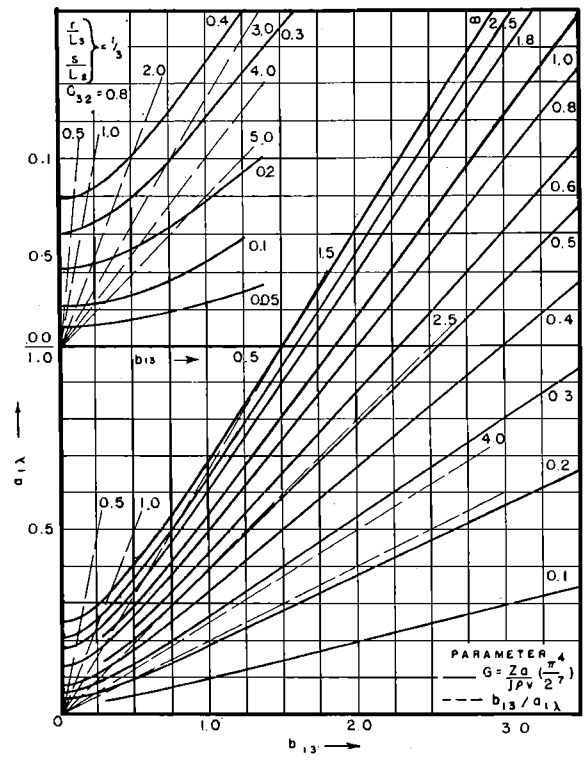

FIG. 4. Design curves, rigid wall at $x=0$.

This is represented by the unbroken lines. The straight broken lines are plotted for various values of the ratio $b_{13}/a_{1\lambda}$ in order to facilitate the use of the graphs in resonant frequency computations. The parameter from sheet to sheet is the ratio $r/L_3=s/L_2$, crystal cross-section dimensions to liquid backing cross-section dimensions. The inserts in the upper left corners consist of expanded portions of the graphs in the neighborhood of $a_{1\lambda}=0$, $b_{13}=0$. The impedance curves given in this paper consist of only the first branch of the impedance function (7b).

In obtaining the resonant frequency of a system, crystal plus backing, it is more convenient to solve for the length of backing needed to obtain a given frequency than to solve for the resonant frequency of a crystal system with a given length of backing. We proceed as follows.

We note that the condition at the first resonant frequency of a crystal system treated one-dimensionally can be written in the form[9]

$$\gamma_c+\alpha=\pi \tag{11}$$

where $\gamma_c=\omega L_c/V_c$ and $\alpha=\tan^{-1}V_a/\rho_c V_c$. L_c is the length of the crystal. The quantity V_a is the input acoustic reactance into the backing material. In general, the velocity V_c in the crystal is dependent on the frequency. This will be discussed later. Let us assume that the first resonant frequency of a free crystal of length L_c is f_0 and that we know the velocity V_c as a function of frequency. After deciding the frequency range of interest and the cross section of the backing material, we compute in the order indicated the following quantities: f/f_0; L_c/λ_c, where $\lambda_c=V_c/f$; γ_c (in degrees), equal to $360\ L_c/\lambda_c$; α (in degrees), equal to $180-\gamma_c$; $\tan\alpha$; $(\pi^4/2^7)(\rho_c V_c/\rho V)$, where ρV is the characteristic impedance of the backing material; G, equal to $(\pi^4/2^7)(\rho_c V_c/\rho V)\tan\alpha$; (V/V_c) where V is the velocity in the backing material; and $b_{13}/a_{1\lambda}$, equal to $(V/V_c)(\lambda_c/L_c)(L_c/L_3)$. The quantity $a_{1\lambda}$ can then be obtained by entering the graphs with the computed values of G and $b_{13}/a_{1\lambda}$. Then L_1/L_c follows, since it is equal to $(V/V_c)(\lambda_c/L_c)a_{1\lambda}$; L_1 is equal to $(L_1/L_c)L_c$. If a thin section of material of thickness L_t and density ρ_2 is interposed between the crystal and the liquid backing, account can be taken of this by diminishing the quantity $\tan\alpha$ by $\rho_2\omega L_t/\rho_c V_c$ in computing the quantity G. We have, thus, obtained the length of backing liquid L_1 required to shift the resonant frequency to a given value. If a curve for a given value of G and a line for a given value of the ratio $b_{13}/a_{1\lambda}$ do not intersect, then the frequency cannot be lowered to the chosen value for any length of the backing liquid, if the cross-section dimensions remain constant.

As the resonant frequency of the system is reduced, the required values of G needed to realize this reduction increase to infinity. For further reduction, the necessary values of G are negative. This implies that the second

[9] See, for example, W. J. Fry, J. M. Taylor, B. W. Henvis, *Design of Crystal Vibrating Systems* (Dover Publications, Inc., New York, 1948), p. 163.

branch of the impedance function (7b) must be used. The graphs of this paper cover the range of values of G from zero to the first infinity.

Case 2.—We next consider a disturbance such that the pressure over the wall containing the crystal is zero, that is, it is a pressure-release surface as are the other five walls. However, over the crystal face, the normal velocity is considered constant. As illustrated in Fig. 7 in the plane $x=0$, over the cross hatched section, $P=0$ and $u_x=C'$ over the center section.

From the expressions (2) and (3) at $x=0$, we have for the n, m mode

$$[P_{nm}]_{x=0}=A_{nm}\sin\frac{n\pi z}{L_3}\sin\frac{m\pi y}{L_3}\sin\left\{-L_1\left[k^2-\left(\frac{n\pi}{L_3}\right)^2-\left(\frac{m\pi}{L_2}\right)^2\right]^{\frac{1}{2}}\right\}, \tag{12a}$$

$$[u_{xnm}]_{x=0}=\frac{j}{\omega\rho}\left(\frac{\partial P}{\partial x}\right)_{x=0}$$

$$=\frac{j}{\omega\rho}A_{nm}\left[k^2-\left(\frac{n\pi}{L_3}\right)^2-\left(\frac{m\pi}{L_2}\right)^2\right]^{\frac{1}{2}}\sin\frac{n\pi z}{L_3}\sin\frac{m\pi y}{L_2}\cos\left\{-L_1\left[k^2-\left(\frac{n\pi}{L_3}\right)^2-\left(\frac{m\pi}{L_2}\right)^2\right]^{\frac{1}{2}}\right\}. \tag{12b}$$

Since we are choosing a real number as the normal velocity amplitude over the crystal face, we note that when the quantity $[k^2-(n\pi/L_3)^2-(m\pi/L_2)^2]^{\frac{1}{2}}$ in (12b) is imaginary, then A_{nm} must be real. Likewise, if $[k^2-(n\pi/L_3)^2-(m\pi/L_2)^2]^{\frac{1}{2}}$ is real, A_{nm} must be imaginary. From this we note that if we let

$$H_{nm}=\frac{j}{\omega\rho}A_{nm}\left[k^2-\left(\frac{n\pi}{L_3}\right)^2-\left(\frac{m\pi}{L_2}\right)^2\right]^{\frac{1}{2}}$$

$$\times\cos\left\{-L_1\left[k^2-\left(\frac{n\pi}{L_3}\right)^2-\left(\frac{m\pi}{L_2}\right)^2\right]^{\frac{1}{2}}\right\}, \tag{13}$$

H_{nm} is always a real quantity. We introduce the quantities

$$G_{nm}=jA_{nm}\sin\{-L_1[k^2-(n\pi/L_3)^2-(m\pi/L_2)^2]^{\frac{1}{2}}\} \tag{14}$$

and

$$\beta_{nm}=\frac{\tan\{-L_1[k^2-(n\pi/L_3)^2-(m\pi/L_2)^2]^{\frac{1}{2}}\}}{[k^2-(n\pi/L_3)^2-(m\pi/L_2)^2]^{\frac{1}{2}}\lambda/\pi}$$

$$=-a_{1\lambda}\tan\pi E_{nm}/E_{nm}. \tag{15}$$

Note that β_{nm} is real. We then have the relation

$$G_{nm}=z\rho V\beta_{nm}H_{nm}, \tag{16}$$

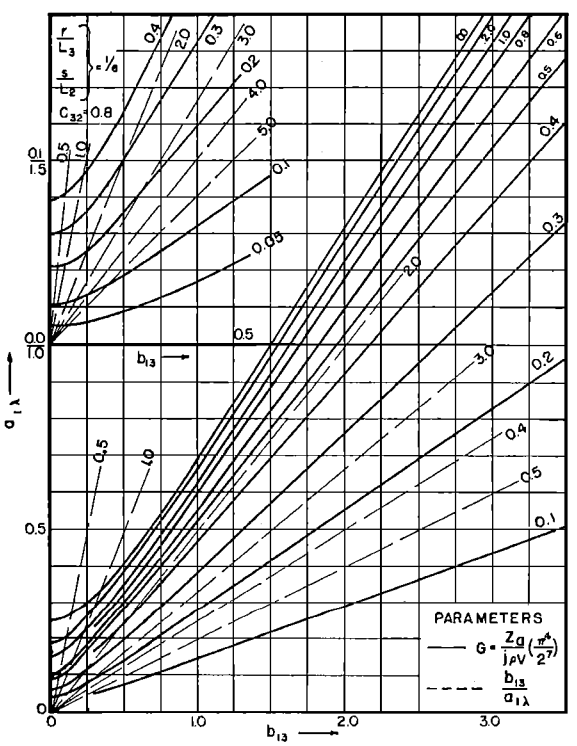

FIG. 5. Design curves, rigid wall at $x=0$.

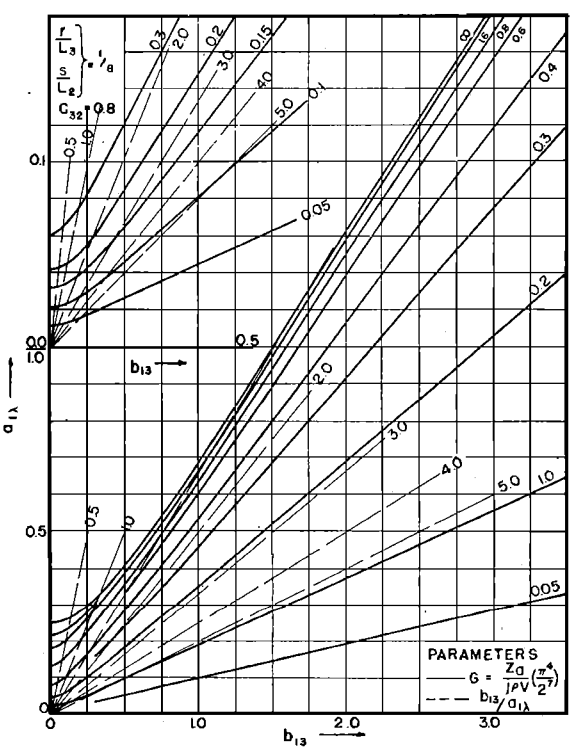

FIG. 6. Design curves, rigid wall at $x=0$.

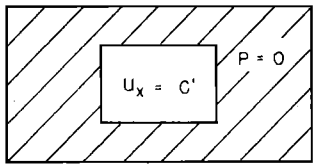

FIG. 7. Boundary conditions in the plane at $x=0$.

where β_{nm}, H_{nm}, and, consequently, G_{nm} are real quantities and n and m are odd integers.

It is convenient to replace H_{nm} and β_{nm} by symbols with but one subscript, as h_l and β_l. In order to realize this, we introduce a correspondence between these symbols as follows:

$$\begin{array}{llll} H_{11} & H_{13} & H_{15} & H_{17} \cdots \\ H_{31} & H_{33} & H_{35} & \cdots \\ H_{51} & H_{53} & \cdots & \\ H_{71} & \cdots & & \\ \cdots & & & \end{array} \qquad \begin{array}{llll} h_1 & h_2 & h_4 & h_7 \cdots \\ h_3 & h_5 & h_8 & \cdots \\ h_6 & h_9 & \cdots & \\ h_{10} & \cdots & & \\ \cdots, & & & \end{array} \tag{17}$$

where symbols in corresponding positions are equivalent. The correspondence between β_{nm} and β_l is identical. We also introduce the notation

$$q_l = \sin(n\pi z/L_3)\sin(m\pi y/L_2)$$

with the same correspondence.

With this notation, we have then

$$P_l = (2\rho V/j)\beta_l h_l q_l, \tag{18a}$$

$$(u_{xl})_{x=0} = h_l q_l. \tag{18b}$$

To obtain a measure of the deviation of P from the value zero over the cross-hatched section Fig. 7, we write

$$\int_\tau [jP_{x=0}(y,z)-0]^2 dydz = \int_\tau [jP_{x=0}(y,z)]^2 dydz, \tag{19}$$

where the integration is over the surface of the supporting wall. Similarly, a measure of the deviation of u_x from C' over the face of the crystal is given by

$$\int_c [(u_x)_{x=0}-C']^2 dydz, \tag{20}$$

where the integration is over the area of the crystal face.

We would like to obtain values h_l which will make these deviations a minimum. Since this cannot, in general, be achieved for both functions simultaneously (that is, for the same values of h_l), we seek a set of h_l which will make the sum of Eqs. (19) and (20) a minimum. From the preceding development, it is observed that the weighting factor $2\rho V\beta_1$ will be of suitable magnitude to use in forming such a sum. We require that

$$(2\rho V\beta_1)^{-2}\int_\tau [jP_{x=0}]^2 dydz + \int_c [(U_x)_{x=0}-C']^2 dydz \tag{21}$$

be a minimum.

Substituting a summation over expression (18a) and (19b) into (21) and interchanging the order of summation and integration, the expression becomes:

$$\frac{1}{\beta_1^2}\sum_l h_l^2\beta_l^2\int_w q_l^2 dydz - \frac{1}{\beta_1^2}\sum_{lk} h_l h_k \beta_l\beta_k \int_c q_l q_k dydz + \sum_{lk} h_l h_k \int_c q_l q_k dydz - 2C'\sum_l h_l \int_c q_l dydz + C'^2\int_c dydz, \tag{22}$$

where the expression (19) has been written as the difference

$$\int_w [jP_{x=0}]^2 dydz - \int_c [jP_{x=0}]^2 dydz, \tag{23}$$

where w implies integration over the total area of the end, Fig. 7.

Introducing the notation

$$\int_c q_l dydz = d_l, \tag{24a}$$

$$\int_w q_l^2 dydz = b_l, \tag{24b}$$

$$\int_c q_l q_k dydz = b_{lk} = b_{kl}, \tag{24c}$$

and collecting terms, expression (22) becomes

$$C'^2\int_c dydz - 2C'\sum_l h_l d_l + (1/\beta_1^2)\sum_l h_l^2\beta_l^2 b_l + \sum_{lk}[1-\beta_l\beta_k/\beta_1^2]h_l h_k b_{lk}. \tag{25}$$

Differentiating with respect to h_r to obtain the values of h_l for a minimum, we find

$$-2C'd_r + (2/\beta_1^2)\beta_r^2 b_r h_r + \sum_k[1-\beta_r\beta_k/\beta_1^2]b_{rk}h_k + \sum_l[1-\beta_l\beta_r/\beta_1^2]b_{lr}h_l = 0. \tag{26}$$

Since by Eq. (24c), $b_{lk}=b_{kl}$, Eq. (26) may be written as

$$(\beta_r^2/\beta_1^2)b_r h_r+\sum_k[1-\beta_r\beta_k/\beta_1^2]b_{rk}h_k=C'd_r, \qquad r=1, 2, 3, \cdots. \quad (27)$$

Letting

$$h_k/c'=h_k' \quad \text{and} \quad [1-\beta_r\beta_k/\beta_1^2]b_{rk}=\alpha_{rk}b_{rk}, \quad (28)$$

we have

$$(\beta_r^2/\beta_1^2)b_r h_r'+\sum_k b_{rk}\alpha_{rk}h_k'=d_r, \quad r=1, 2, 3, \cdots, \quad (29)$$

which may be written as the array

$$\begin{aligned}
&[\alpha_{11}b_{11}+(\beta_1^2/\beta_1^2)b_1]h_1'+\alpha_{12}b_{12}h_2'+\alpha_{13}b_{13}h_3' &&\\
&\qquad +\cdots=d_1,\\
&\alpha_{21}b_{21}h_1'+[\alpha_{22}b_{22}+(\beta_2^2/\beta_1^2)b_2]h_2'+\alpha_{23}b_{23}h_3' &&\\
&\qquad +\cdots=d_2, \quad (30)\\
&\alpha_{31}b_{31}h_1'+\alpha_{32}b_{32}h_2'+[\alpha_{33}b_{33}+(\beta_3^2/\beta_1^2)b_3]h_3' &&\\
&\qquad +\cdots=d_3,\\
&\quad\cdots
\end{aligned}$$

where the coefficients are tabulated below.

When $n=i$, $m=j$,

$$\frac{b_{rk}}{L_2L_3}=\left[\frac{r}{L_3}+\left(\frac{1}{2n\pi}\right)\sin\frac{2n\pi r}{L_3}\right]\left[\frac{s}{L_2}+\left(\frac{1}{2m\pi}\right)\sin\frac{2m\pi s}{L_2}\right];$$

when $m=j$, $n\neq i$,

$$\frac{b_{rk}}{L_2L_3}=\frac{1}{\pi}\left[\frac{s}{L_2}+\left(\frac{1}{2m\pi}\right)\sin\frac{2m\pi s}{L_2}\right]\left[\frac{(-1)^{\frac{1}{2}(n-i)}}{n-i}\sin(n-i)\frac{\pi r}{L_3}-\frac{(-1)^{\frac{1}{2}(n+i)}}{n+i}\sin(n+i)\frac{\pi r}{L_3}\right];$$

when $m\neq j$, $n=i$,

$$\frac{b_{rk}}{L_2L_3}=\frac{1}{\pi}\left[\frac{r}{L_3}+\left(\frac{1}{2n\pi}\right)\sin\frac{2n\pi r}{L_3}\right]\left[\frac{(-1)^{\frac{1}{2}(m-j)}}{m-j}\sin(m-j)\frac{\pi s}{L_2}-\frac{(-1)^{\frac{1}{2}(m+j)}}{m+j}\sin(m+j)\frac{\pi s}{L_2}\right];$$

when $m\neq j$, $n\neq i$,

$$\frac{b_{rk}}{L_2L_3}=\frac{1}{\pi^2}\left[\frac{(-1)^{\frac{1}{2}(m-j)}}{m-j}\sin(m-j)\frac{\pi s}{L_2}-\frac{(-1)^{\frac{1}{2}(m+j)}}{m+j}\sin(m+j)\frac{\pi s}{L_2}\right]\left[\frac{(-1)^{\frac{1}{2}(n-i)}}{n-i}\sin(n-i)\frac{\pi r}{L_3}-\frac{(-1)^{\frac{1}{2}(n+i)}}{n+i}\sin(n+i)\frac{\pi r}{L_3}\right].$$

The average input acoustic impedance into the backing liquid is given by the ratio of the average pressure, $\bar{P}$, and the normal component of the particle velocity, C',

$$Z_a=\bar{P}/C'=(1/4rsC')\int_{\frac{1}{2}L_3-r}^{\frac{1}{2}L_3+r}\int_{\frac{1}{2}L_2-s}^{\frac{1}{2}L_2+s}P\,dy\,dz. \quad (31)$$

In terms of symbols defined above and the variables h_l' of Eq. (30), this relation for Z_a can be expressed as

$$Z_a=j\rho V\left(\frac{2L_2L_3}{rs}\right)\left(\frac{a_{1\lambda}}{\pi^2}\right)\sum_{nm}h_l'(-1)^{\frac{1}{2}(n+m-2)}\sin\frac{n\pi r}{L_3}\sin\frac{m\pi s}{L_2}\frac{\tan\pi E_{nm}}{nmE_{nm}}, \quad (32)$$

where the values of the subscript l, corresponding to a pair of values of n and m, are given by the correspondence indicated in Eq. (17).

We observe that as b_{13} approaches zero, that is, if the cross-sectional dimensions of the liquid backing become large, the length L_1 and the wavelength λ remaining constant, Eq. (30) reduces to a simple diagonal form. The quantity $\alpha_{rk}\to 0$ and $\beta_i^2/\beta_1^2\to 1$, and the equations become,

$$h_j'=d_j/b_j, \quad j=1, 2, 3, \cdots. \quad (33)$$

The expression for the input acoustic impedance (32) reduces to that obtained in Case 1 when $b_{13}\to 0$, i.e., relation (10).

The results of a computation of the input acoustic impedance, formula (32), are presented in graphical form in Fig. 8 for a range of values of $a_{1\lambda}$ and b_{13}. The ratios r/L_3 and s/L_2 are equal to $\frac{1}{4}$, which correspond to cross-section dimensions of the backing liquid twice the size of the opening. The parameters for the two sets of curves are $G'=(Z_a/j\rho V)(\pi^2/2^4)$ and $b_{13}/a_{1\lambda}$. Note that the multiplicative constant $(\pi^2/2^4)$ in the definition of G' differs from that in G.

The predicted variation of the resonant frequency of an ADP crystal $\frac{5}{8}$ in. long and $\frac{1}{2}\times\frac{5}{8}$ inch in cross-section dimensions as a function of the ratio of the length L_1 of the mercury backing to the length L_c of the crystal is shown graphically in Fig. 9. The cross-section dimensions of the backing liquid are $1\frac{1}{4}\times 1$ in. The solid curve is obtained from the theory developed under Case 1 and the dashed curve is obtained on the basis of the theory of Case 2. This graph shows that for cross-section dimensions twice those of the opening the rigid end case approximates closely the pressure-release case as far as the variation of the resonant frequency with

length of backing is concerned. This is convenient from the point of view of design, since the amount of calculation required in utilizing the theory for the pressure-release end is greatly in excess of that required when using the theory for the rigid end.

2. Loss

We now consider briefly the various loss factors associated with these variable resonant frequency crystal systems. As indicated in the introduction, these loss factors determine the resistive component of the acoustic impedance of the load on the crystal. The quality factor, Q', can then be obtained from the following approximate relation:[10]

$$Q' \sim (\theta/X_a)^2[(\cos\gamma_0 - 1)/\cos\gamma_0]^4, \qquad (34)$$

where X_a is the ratio of the resistive component of the acoustic impedance of the load and the characteristic impedance of the crystal ($\rho_c V_c$). The quantity γ_0 is equal to $2\pi f_0 L_c/V_c$, where f_0 is the calculated value of the resonant frequency of the crystal system under no loss conditions. The quantity θ is given by $\theta = \varphi^2/A_c\rho_c V_c(V_c/L_c)C_0\gamma_0$, where C_0 is the clamped capacity of the crystal, and A_c is the area of the crystal face in contact with the backing. The quantity φ is given by $\varphi = (d/s)l_w$ for longitudinal modes, $\varphi = (d/s)(A_c/L_c)$ for thickness modes. Values of the ratio (d/s) for various crystal cuts can be obtained from the literature.[9]

A. Internal Losses in the Crystals

At the present time, there are available piezoelectric crystals which have high electromechanical coupling coefficients for longitudinal or thickness modes and which have relatively low internal loss coefficients as compared to other components of the crystal system. Therefore, we will neglect this source of loss.

B. Interface Losses

We next consider the loss of acoustical energy at the interface between the liquid backing material and the walls of the supporting container, that is, at the liquid-decoupling material interface. It will be assumed that the losses are small in order that the following approximate method of analysis will yield a suitable relation.

The boundary condition for the no-loss development treated above is $P=0$ at the container-interface. This condition leads to an expression for particle velocity which has tangential components at the interface equal to zero. We now assume that the expression for the normal component of the particle velocity u_n at the walls for the no loss case is approximately equal to that for the case of loss. This velocity component, u_n, is expressible in terms of pressure as $u_n = (j/\omega\rho)\partial P/\partial n$, where n designates the particular coordinate variable of interest, that is either x, y, or z. The positive direction of u_n is in the positive direction of the corresponding coordinate axis.

[10] R. B. Fry and W. J. Fry, J. App. Phys. (to be published).

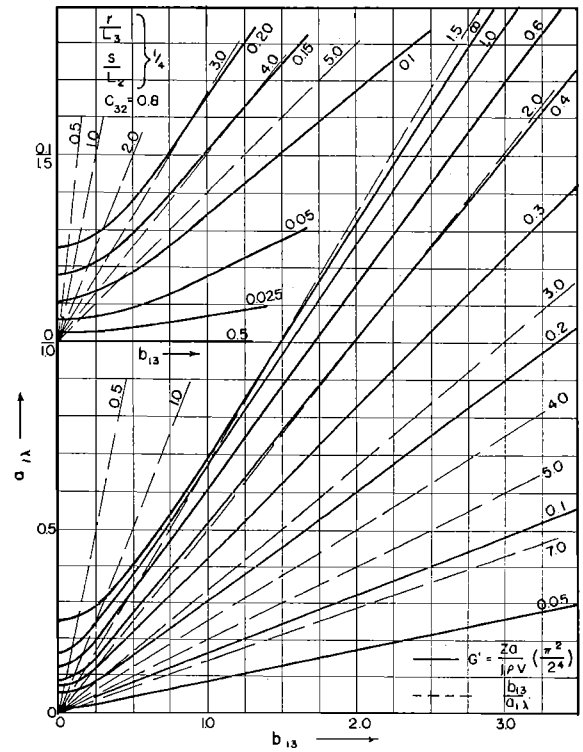

FIG. 8. Design curves, pressure release wall at $x=0$.

We now characterize the wall by a normal acoustical impedance of pure resistive type, that is, $P/U_n' = R_{aw}$, where P is the sound pressure amplitude at the interface and U_n' is the normal particle velocity amplitude positive direction into the wall. We can designate R_{aw} as the input resistance of the wall per unit area. The energy lost to the wall per unit area per second is then

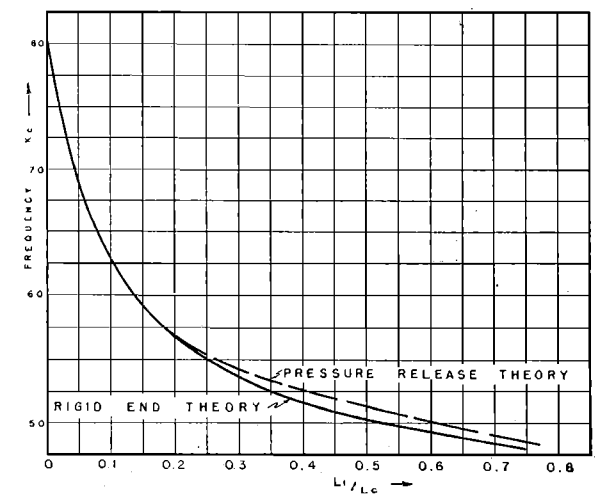

FIG. 9. Comparison of theoretical results for the variation of the resonant frequency as a function of the ratio L_1/L_c for two different boundary conditions in the plane $x=0$.

$\frac{1}{2}|U_n'|^2R_{aw}$. This expression is identical with $\frac{1}{2}u_n^2R_{aw}$, since u_n is a pure real number (expressions (3) and (12b)). The total energy lost per second is then

$$\tfrac{1}{2}\int R_{aw}u_n^2 d\sigma, \tag{35}$$

where the integration is carried out over all walls of the confining vessel which contribute to the loss.

Expression (35) for the power loss enables us to obtain an expression for the mechanical input resistance into the backing liquid looking in at the coupling material-backing liquid interface. (See Fig. 1.) If we designate this mechanical impedance by R_{mb} and let the particle velocity amplitude at this interface be C', we obtain for the energy transferred into the backing liquid the expression $\frac{1}{2}C'^2R_{mb}$. But this energy is equal to the energy as given by expression (35). Therefore,

$$R_{mb}=(R_{aw}/C'^2)\int u_n^2 d\sigma, \tag{36}$$

where we assume that R_{aw} is constant for all the walls and the integration is carried out over all the walls.

This integral yields the following relation for R_{mb} for Case 1. (We assume no loss at the rigid wall.)

$$\frac{R_{mb}/L_2L_3}{2\,{}^8R_{aw}/\pi^5}=\frac{\pi}{2^2}\sum_{nm}\frac{\sin^2(m\pi s/L_2)\sin^2(n\pi r/L_3)}{n^2m^2\cos^2\pi E_{nm}}$$

$$+b_{13}\sum_{\substack{nmi\\ n\neq i}}\frac{(-1)^{\frac{1}{2}(n+i+2)}}{m^2(i^2-n^2)}\sin^2\frac{m\pi s}{L_2}\sin\frac{n\pi r}{L_3}\sin\frac{i\pi r}{L_3}\left(\frac{\tan\pi E_{nm}}{E_{nm}}-\frac{\tan\pi E_{im}}{E_{im}}\right)$$

$$+\frac{b_{13}{}^3}{2}\sum_{nm}\frac{\sin^2(m\pi s/L_2)\sin^2(n\pi r/L_3)}{m^2E_{nm}{}^2}\left(\frac{\pi}{\cos^2\pi E_{nm}}-\frac{\tan\pi E_{nm}}{E_{nm}}\right)$$

$$+b_{13}c_{32}\sum_{\substack{nmj\\ m\neq j}}\frac{(-1)^{\frac{1}{2}(m+j+2)}}{n^2(j^2-m^2)}\sin^2\frac{n\pi r}{L_3}\sin\frac{m\pi s}{L_2}\sin\frac{j\pi s}{L_2}\left(\frac{\tan\pi E_{nm}}{E_{nm}}-\frac{\tan\pi E_{nj}}{E_{nj}}\right)$$

$$+\frac{(b_{13}c_{32})^3}{2}\sum_{nm}\frac{\sin^2(m\pi s/L_2)\sin^2(n\pi r/L_3)}{n^2E_{nm}{}^2}\left(\frac{\pi}{\cos^2\pi E_{nm}}-\frac{\tan\pi E_{nm}}{E_{nm}}\right). \tag{37}$$

For Case 2, the integral becomes

$$\frac{R_{aw}}{\rho^2\omega^2C'^2}\left\{\sum_{nm}A_{nm}{}^2\left(\frac{\pi^2}{c_{32}b_{13}{}^2}\right)E_{nm}{}^2\cos^2\pi E_{nm}\left\{\frac{1}{2^2}-\left[\frac{r}{L_3}+\frac{\sin(2n\pi r/L_3)}{2n\pi}\right]\left[\frac{s}{L_2}+\frac{\sin(2m\pi s/L_2)}{2m\pi}\right]\right\}\right.$$

$$-\sum_{\substack{nmij\\ n\neq i,\ m\neq j}}A_{nm}A_{ij}\left(\frac{1}{c_{32}b_{13}{}^2}\right)E_{nm}E_{ij}\cos\pi E_{nm}\cos\pi E_{ij}$$

$$\times\left[\frac{(-1)^{\frac{1}{2}(n-i)}}{n-i}\sin(n-i)\frac{\pi r}{L_3}-\frac{(-1)^{\frac{1}{2}(n+i)}}{n+i}\sin(n+i)\frac{\pi r}{L_3}\right]\left[\frac{(-1)^{\frac{1}{2}(m-j)}}{m-j}\sin(m-j)\frac{\pi s}{L_2}-\frac{(-1)^{\frac{1}{2}(m+j)}}{m+j}\sin(m+j)\frac{\pi s}{L_2}\right]$$

$$-\sum_{\substack{nmj\\ m\neq j}}A_{nm}A_{nj}\left(\frac{\pi}{c_{32}b_{13}{}^2}\right)E_{nm}E_{nj}\cos\pi E_{nm}\cos\pi E_{nj}$$

$$\times\left[\frac{r}{L_3}+\frac{\sin(2n\pi r/L_3)}{2n\pi}\right]\left[\frac{(-1)^{\frac{1}{2}(m-j)}}{m-j}\sin(m-j)\frac{\pi s}{L_2}-\frac{(-1)^{\frac{1}{2}(m+j)}}{m+j}\sin(m+j)\frac{\pi s}{L_2}\right]$$

$$-\sum_{\substack{nmi\\ n\neq i}}A_{nm}A_{im}\left(\frac{\pi}{c_{32}b_{13}{}^2}\right)E_{nm}E_{im}\cos\pi E_{nm}\cos\pi E_{im}$$

$$\left.\times\left[\frac{(-1)^{\frac{1}{2}(n-i)}}{n-i}\sin(n-i)\frac{\pi r}{L_3}-\frac{(-1)^{\frac{1}{2}(n+i)}}{n+i}\sin(n+i)\frac{\pi r}{L_3}\right]\left[\frac{s}{L_2}+\frac{\sin(2m\pi s/L_2)}{2m\pi}\right]\right\}. \tag{38}$$

C. Volume Loss

It is readily shown that the volume losses in the liquid backing in the present experimental variable resonant frequency systems do not contribute appreciably to the loss. An approximate calculation yields values of the quality factor as determined by this loss factor of the order of 10^8. Experimental values are less than 10^3.

Another source of loss of the volume type is in the bonding material between the crystal and the coupling material. The thickness, Δl, of this material is usually small so that we obtain for the absorbed energy the expression

$$E_b=[\alpha_b(\Delta l)/\rho V]\int P^2 ds, \tag{39}$$

where the integration is carried out over the crystal face.

D. Support Losses

The last source of loss which we will consider is that at the supports for the crystal unit. Since it is of primary interest to analyze the losses of a nonradiating system, we will consider only that loss which occurs at the supporting wall for the crystal unit. Losses occurring at the radiating face of the unit are unavoidable only when the unit is used to obtain radiation by coupling to a medium. Under such conditions, the radiation loss usually far outweighs the support loss at the radiating end of the unit. Internal bonding losses occur in a multiple crystal assembly. Such assemblies are of interest primarily at the lower frequencies because longitudinal modes of the piezoelectric elements are used. In this frequency range where longitudinal modes are conveniently used, it has been possible experimentally to keep these losses to a relative low value.

Consider the crystal mounted on a supporting wall as indicated in Fig. 1. As mentioned previously, we are assuming that the velocity amplitude over the crystal face in contact with the backing is a constant, C'. We now assume that the force in the x direction exerted by the supporting wall on the crystal is of the form $-R_f L_p C'$, where R_f is a positive constant, and L_p is the perimeter of the crystal unit in contact with the wall.

Then the loss per second, E_s, in vibrational energy occurring at the supports is given by

$$E_s=\tfrac{1}{2}R_f L_p C'^2. \tag{40}$$

E. Quality Factor

We have presented in the previous sections expressions for the losses in the components of a variable resonant frequency crystal system. In order to evaluate the quality factor of such a system, it is necessary to express these losses in terms of the resistive component of the mechanical impedance of the load on the crystal unit. Now the relation between the input resistance and

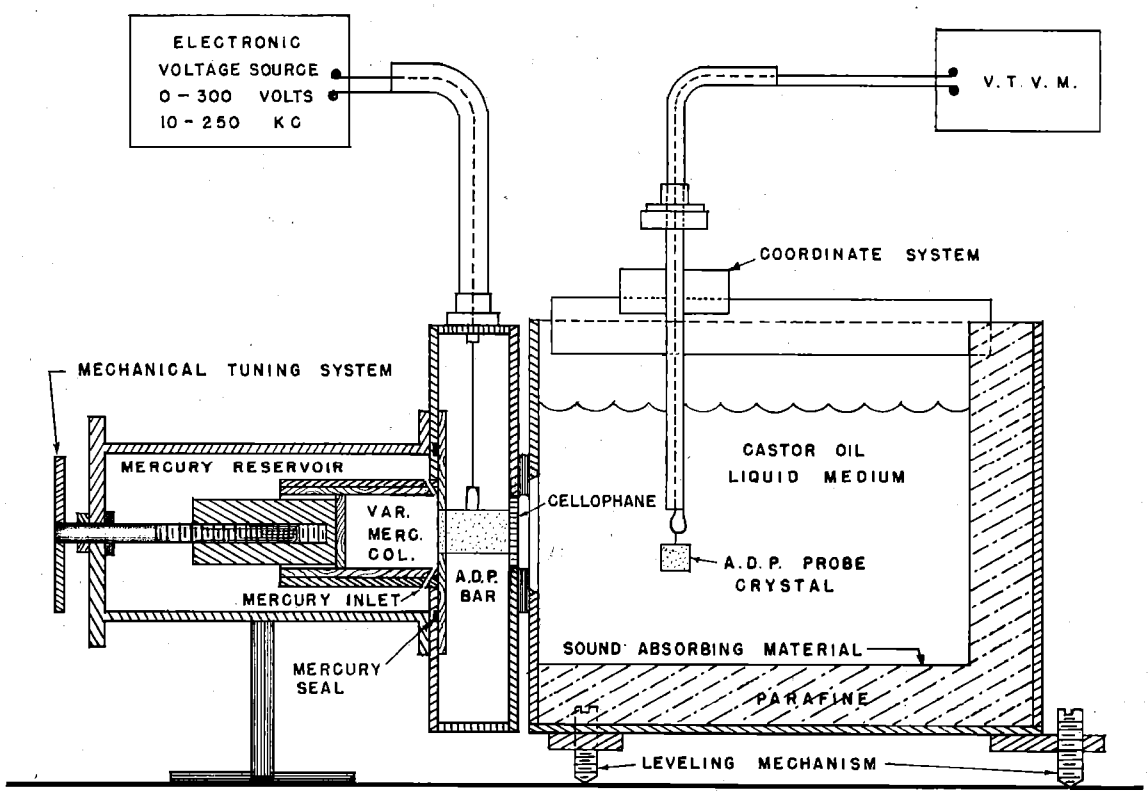

FIG. 10. Diagram of the over-all experimental arrangement.

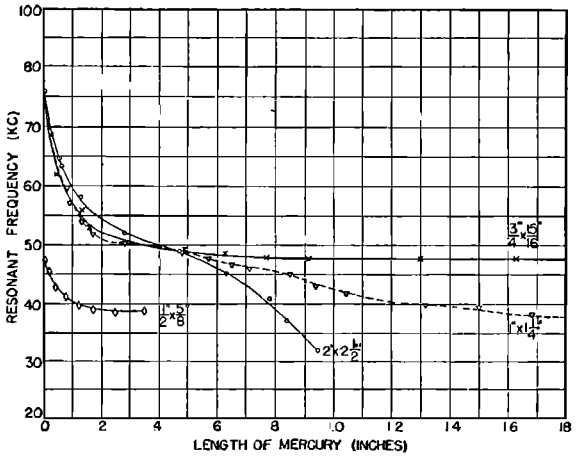

FIG. 11. The effect of various mercury column cross sections and lengths on the reduction of the resonant frequency of a crystal system. The parameter is the cross-sectional dimensions of the mercury column.

the energy transformed is

$$\sum E_i = \tfrac{1}{2} C'^2 R_m, \qquad (41)$$

where $\sum E_i$ indicates a summation over all sources of energy loss. The input resistance is thus

$$R_m = 2[(E_i/C'^2)+(E_b/C'^2)+(E_s/C'^2)], \qquad (42)$$

where E_i is the energy lost at the interfaces between the backing liquid and its supporting container given by expression (35), E_b is that lost in the bonding material (39), and E_s is that lost at the supporting wall (40). A term for the energy lost in the backing liquid would also be included in Eq. (42) if that source of loss were not negligible. The quality factor then follows from relation (34).

III. EXPERIMENT

We now consider the experimental results. We are concerned with the effect of the geometry of the mercury backing on the resonant frequency, the total frequency range, the quality factor, Q', and the acoustic output as a function of the frequency. Figure 10 indicates the arrangement when a variable resonant frequency unit is used to obtain ultrasound in a liquid medium.

The effect of changes in the geometry of the mercury backing was studied by observing the reduction in resonant frequency and the variation in the quality factor as a function of the length of the variable column and as a function of the ratio of crystal cross-sectional area to backing cross-sectional area. In each experiment, the cross section of the column remained constant and the length was changed. Results of these tests are shown in graphical form in Fig. 11. In these comparison experiments, the crystal unit consisted of a single 45° Z cut ADP crystal $\frac{1}{2}\times\frac{5}{8}$ inch in cross-section dimensions. The length of the crystal was 1 in. for the case in which the backing cross-section dimensions were equal to the crystal cross-section dimensions. The resonant frequency of such a free crystal is 60 kc. In all other cases, the crystal unit was $\frac{5}{8}$ in. long, which corresponds to a resonant frequency of 78 kc. One further difference is the thickness of the coupling plate: for the equal cross-section case $\frac{1}{16}$-in. brass was used, and for the others 0.005-in. Ag-Pd alloy was used.

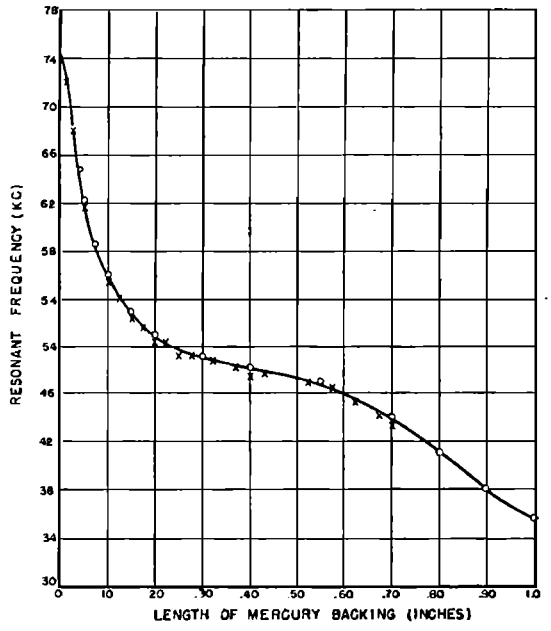

FIG. 12. Resonant frequency *versus* length of mercury backing for a $\frac{1}{2}\times\frac{5}{8}\times\frac{5}{8}$-in. ADP crystal, not radiating.

The curves of Fig. 11 show that the total shift possible with each particular system increases as the cross-section of the mercury increases. This is in line

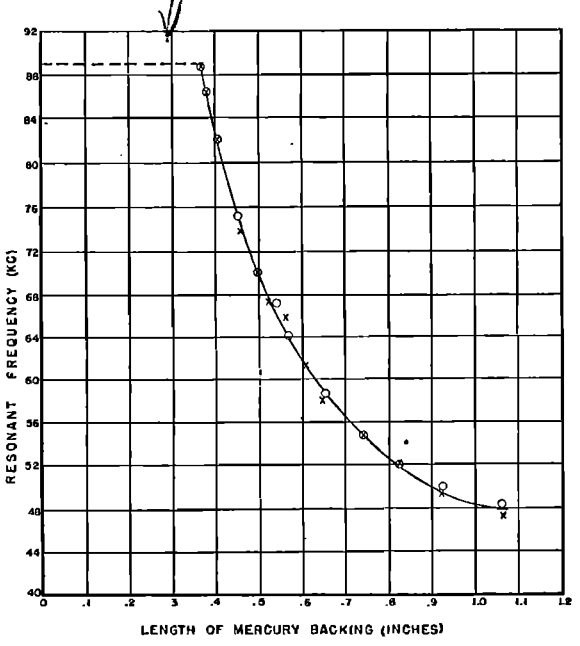

FIG. 13. Resonant frequency *versus* length of mercury backing for a system radiating into a castor oil medium.

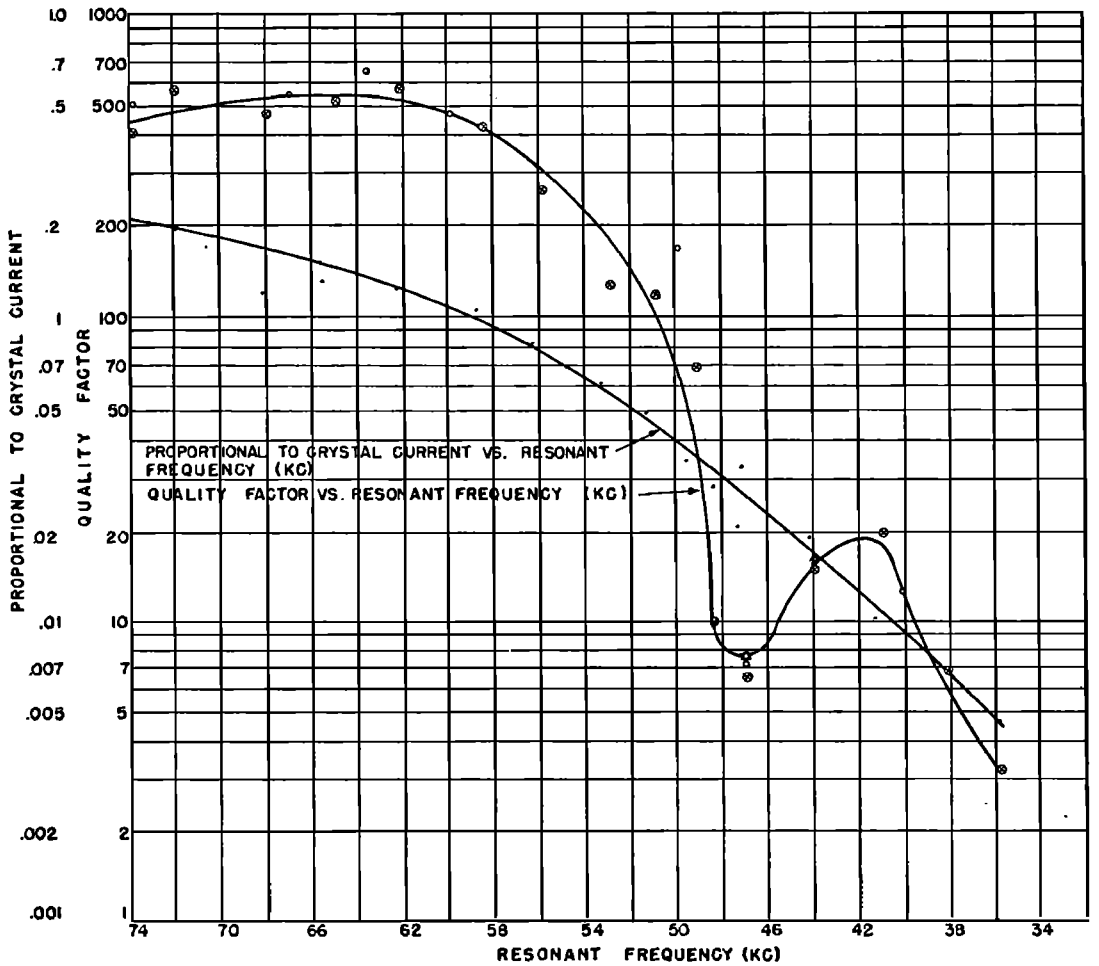

FIG. 14. The change in quality factor and the relative crystal current at resonance as a function of the resonant frequency of a variable resonant frequency system.

with the theoretical result that a tube of liquid with pressure release walls exhibits a cut-off frequency.[4] The quality factor at the maximum resonant frequency shift is approximately 1.5 for all of the systems with the exception of the equal cross-section case. The maximum length of mercury column for this system was 0.4 in., and Q' was 46.5 at the lowest frequency. At this frequency the slope of the curve is close to zero, indicating that the greatest possible reduction in frequency has been almost attained.

Data illustrating the reproducibility of the relation between resonant frequency and mercury column length are shown in Fig. 12 and in Fig. 13 for a large ratio of cross-section area of backing to crystal. The data of Fig. 12 were obtained on the nonradiating (air) system. The results of Fig. 13 apply to the system when it is radiating into a castor oil medium.

Consider first the nonradiating case. It can be seen that an initial rapid drop-off takes place. One-tenth of an inch of mercury produces a 24 percent reduction in the resonant frequency. The next one-tenth of an inch increases the total shift to 31 percent, whereas, 1 in. of mercury is required to produce a shift of 50.5 percent or a frequency change of 2:1. The crystal dimensions for this study were $\frac{1}{2}\times\frac{5}{8}\times\frac{5}{8}$ in. and the cross section of the mercury column was $2\times2\frac{1}{2}$ in. The difference between this curve and the one presented in Fig. 11 for a $2\times2\frac{1}{2}$-in. backing cross-section is probably the result of the addition of a cellophane diaphragm to the front end of the crystal for coupling the system to a castor oil bath. Clamping and alignment may also account for part of the difference.

The curve of Fig. 13 is a typical set of data for the system just discussed when it is coupled to a castor oil medium. The two sets of points illustrate the reproducibility. The length of mercury necessary to reduce the resonant frequency a given amount is different when the system is coupled to a liquid medium. The addition of the liquid complicates the resonant frequency picture. The resonant frequency for the mode of interest is not reduced for the first 0.375 in. of mercury; however, for each increment in the mercury column after this point, the frequency is reduced. This is true until a length of 1.06 in. is reached. For lengths greater than 1.06 in., multiple resonant frequencies appear and the reduction is not as clearly defined. The difference in the highest resonant frequency present for the two loading conditions is of importance. The experimental results demon-

strate that better operational characteristics are obtained over a 2:1 frequency band by utilizing the frequency range from 88.5 kc to 46.5 kc when the system is radiating into a liquid medium.

Figure 14 illustrates the change in quality factor and the relative crystal current at resonance as a function of the resonant frequency of the system under nonradiating conditions. The unit under consideration contains a $\frac{1}{2}\times\frac{5}{8}\times\frac{5}{8}$-in. ADP crystal whose fundamental resonant frequency when completely mounted is 74 kc.

The measured quality factors at the higher frequencies of the band covered by this system are of the order of 450. They remain at this high level for the first 22 percent shift. This characteristic suggests that such systems might be developed for applications other than the production of high intensity ultrasound. A comprehensive study of such characteristics as temperature dependence and stability would be necessary before this could accomplished.

As the resonant frequency is shifted beyond the first 22 percent, the quality factor, Q', decreases rapidly with a minimum occurring at 47 kc. The lowest quality factor is 3 at 50 percent frequency shift. The minimum in the quality factor curve is the result of a decrease in the antiresonant impedance. This is clear from an examination of the curve of crystal current at resonance as a function of resonant frequency. The plotted values of the crystal current are inversely proportional to the resonant impedance. This curve contains no minimum in the neighborhood of 47 kc.

Measurements were made in the sound tank to determine the variation of acoustical output as the resonant frequency of the system was changed. The sound pressure, at various points in the liquid medium, was determined by a probe crystal as previously discussed. The graph of Fig. 15 shows that the acoustic output (in terms of pressure) of the projector is a linear function of the driving voltage over the range investigated. It should be noted that the data are limited to intermediate acoustical power outputs. The peak voltage applied, 1400 v, does not represent a maximum driving voltage for the projector crystal.

The sound pressure amplitude as a function of the resonant frequency is of particular interest. Figure 16a shows a plot of probe voltage as a function of the resonant frequency of the projector for constant driving voltage. The probe voltage decreases by a factor of 7.3 as the resonant frequency changes from 82 kc to 46 kc. An experimental comparison between fixed resonant frequency systems and a variable resonant frequency system is desirable. This can be accomplished by using a set of fixed frequency projectors whose resonant frequencies are distributed through the band covered by the variable unit. The geometry of the complete projector-probe system is held fixed during such a comparison so that changes in sound field distribution will not

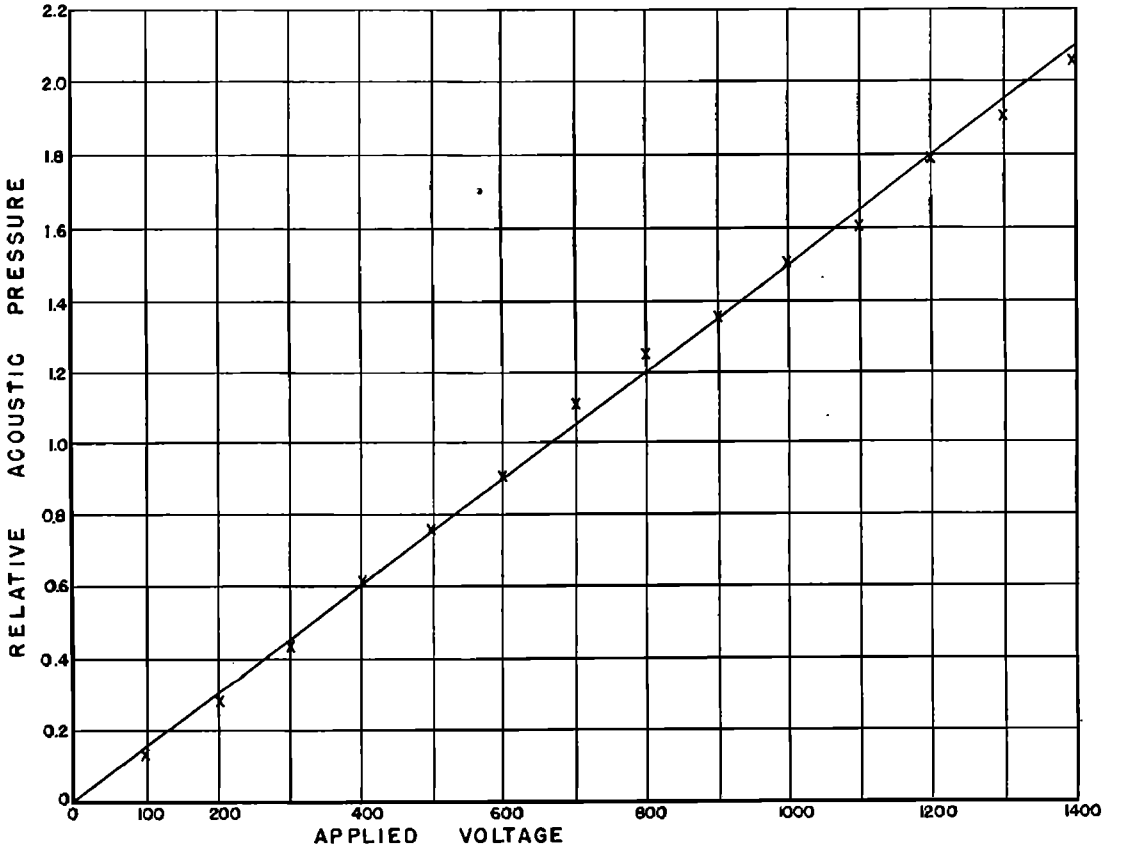

FIG. 15. Applied voltage *versus* relative acoustic pressure amplitude for a variable resonant frequency crystal system radiating into a liquid medium.

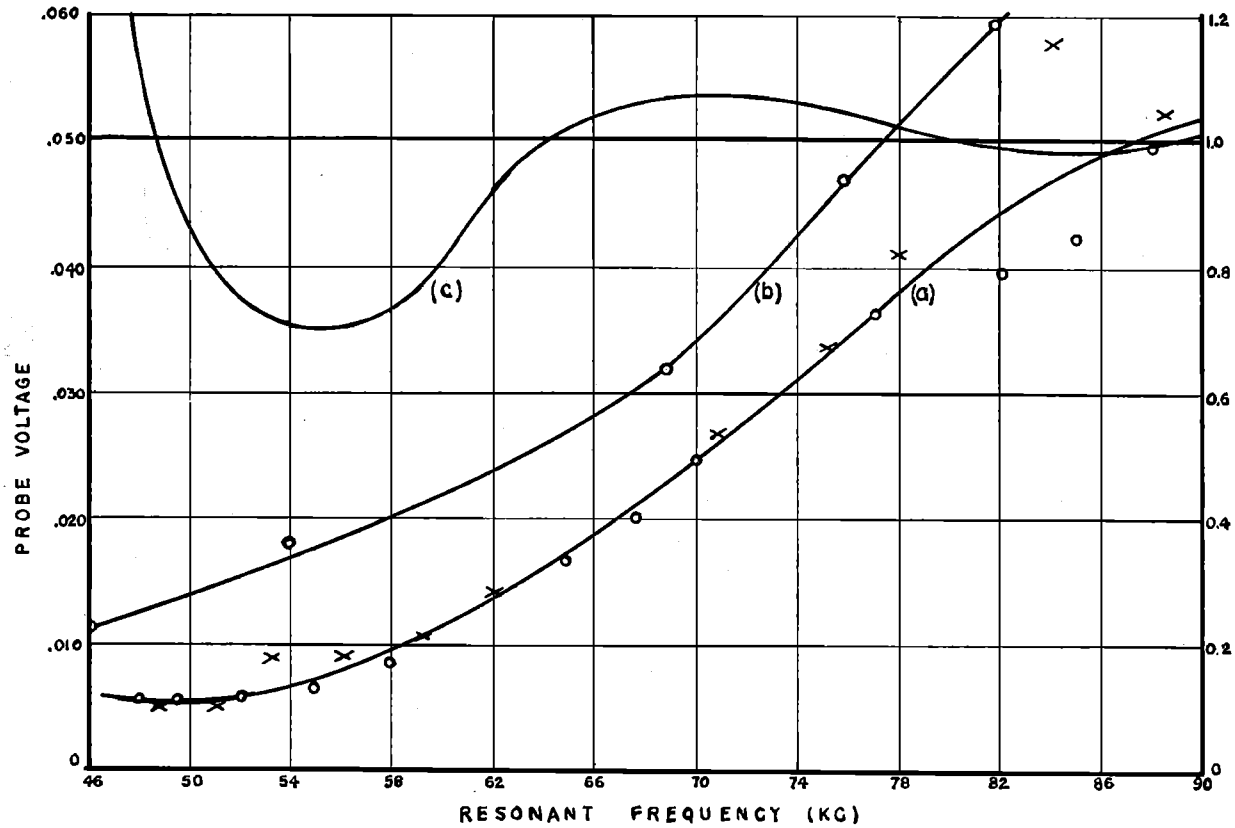

FIG. 16. (a) Probe voltage *versus* resonant frequency for a variable resonant frequency unit under constant driving voltage. (b) Probe voltage *versus* resonant frequency for five fixed frequency units. (c) A graphical comparison of the acoustic outputs of fixed and a variable resonant frequency system.

influence the results. Data collected using five fixed resonant frequency units are shown in Fig. 16b. The sound pressure decrease for these units is 5.4 over the same frequency range covered by the variable resonant frequency system.

A graphical comparison of the two systems can be made as indicated in Fig. 16c. For the figure, the output of both systems was arbitrarily chosen as unity at 82 kc, and the data at other frequencies were referred to this base. It should be pointed out that this graph is not plotted as a comparison of absolute pressure amplitudes, since the output of the variable frequency unit is approximately 0.8 that of the fixed frequency unit at 82 kc. From this comparison, it is clear that the power output, for equal values of the driving electric field, of a variable resonant frequency unit is roughly equal to the power output of a fixed resonant frequency unit operating at the same frequency. This statement applies throughout the 2:1 frequency band covered by the variable unit.

IV. COMPARISONS

In order to compare the results of theory with experimental values, we consider specific examples. We first choose as the piezoelectric element a single 45° Z cut ammonium dihydrogen phosphate (ADP) crystal 1 in. long and $\frac{1}{2}\times\frac{5}{8}$ inch in cross-section. The distance between electroded faces is $\frac{1}{2}$ in. The first resonant frequency of such a crystal is about 60 kc. If we insert the values for the length, $L_c=1.0$ in., and the resonant frequency into the relation $\omega L_c/V_c=\pi$ (the condition for the first resonant frequency derived on the basis of a one dimensional theory for the vibrating crystal),[9] we obtain a value for the velocity V_c in the crystal. To obtain values for the velocity V_c in the crystal at resonant frequencies characteristic of the composite system, crystal plus backing, we simply assume that such velocities are equal to the velocities computed from the relation $\omega L_c/V_c=\pi$, where L_c is the length of free crystal necessary to obtain a frequency equal to the frequency of the composite system for a particular length of backing material. The cross-sectional dimensions of the crystal used for obtaining values of V_c are equal to those of the crystal which is terminated with the backing material. The necessary data for ADP crystals are contained, for example, in reference 9, p. 12. If one plots the "effective velocity V_c" in a crystal $\frac{5}{8}$ in. wide as a function of frequency, using the data in the reference just cited, one obtains the graph of Fig. 17.

If the 1.0-in. crystal is coupled to a backing liquid of mercury, equal in cross-section dimensions to those of the crystal, through a $\frac{1}{16}$-in. brass plate, one obtains the experimental values indicated by crosses in Fig. 18 for the resonant frequency of the composite system as a

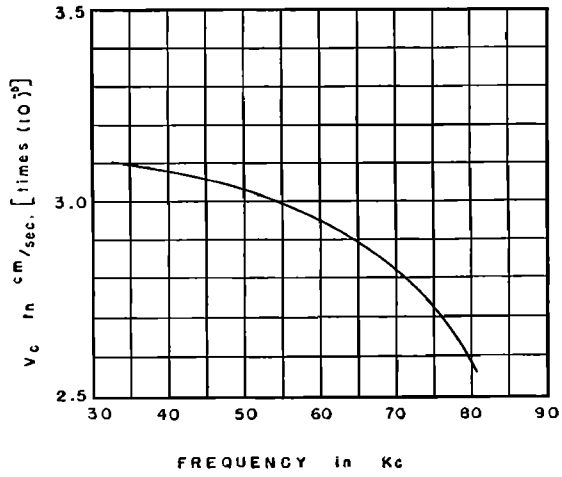

FIG. 17. "Effective sound velocity" in the crystal as a function of frequency.

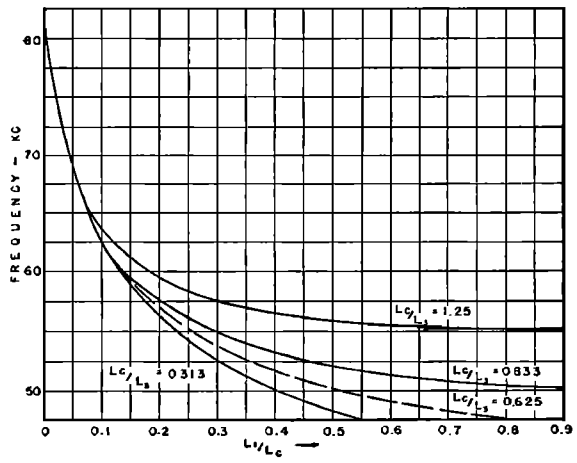

FIG. 19. Theoretical results showing the effect of various cross-section dimensions of a mercury backing on the variation of the resonant frequency with length of mercury backing.

function of the ratio of the length of the mercury backing, L_1, to the length of the crystal, L_c. The curve in Fig. 18 is a graph of the theoretical values. Experimentally, the maximum shift in the resonant frequency obtainable with this system is about 23 percent of the highest frequency (48.4 kc). Theoretically, the maximum shift was computed to be about 21 percent.

The effect of different cross-section sizes of the backing liquid on the relationship between resonant frequency and length of mercury backing is illustrated by the theoretical curves of Fig. 19. The crystal cross-section size is again $\frac{1}{2}\times\frac{5}{8}$ in., but the crystal length is now $\frac{5}{8}$ in. This corresponds to a resonant frequency of the free crystal of about 80 kc. Since the crystal width is $\frac{5}{8}$ in., the curve of Fig. 17 can be used to obtain the velocity V_c as a function of the frequency. Four different curves are shown corresponding to four ratios of cross-section dimensions between the crystal and the backing liquid. The quantity L_c/L_3 is the ratio of the length of the crystal to the shorter of the cross-section dimensions of the mercury backing. The four ratios of linear dimensions are: 1:1, 2:3, 1:2, 1:4. The maximum shift in frequency for the equal cross-section case, $L_c/L_3=1.25$, is about 32 percent and the maximum shift for the 2:3 cross-section case, $L_c/L_3=0.833$, is about 40 percent. These values are obtained under the assumption that the thickness of the coupling material between the crystal and the mercury backing is very small. The curves are obtained, with the exception of the equal cross-section case, on the basis of a theory which assumes that the wall in which the crystal is mounted and which bounds the mercury is rigid. Experimentally, all walls including this one are pressure release surfaces. However, the experimental values lie very close to these curves. Comparison with Fig. 11, which contains experimental curves, indicates general agreement between calculated values and experimental results. It is an advantage from the viewpoint of numerical computation to be able to use the theory which assumes that the wall in which the crystal is mounted is rigid in order to predict the experimental

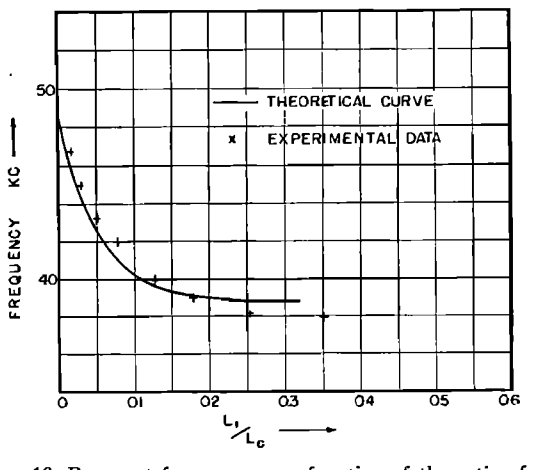

FIG. 18. Resonant frequency as a function of the ratio of the length of mercury backing, L_1, to the length of the crystal L_c. Comparison of the theoretical results with experimental values.

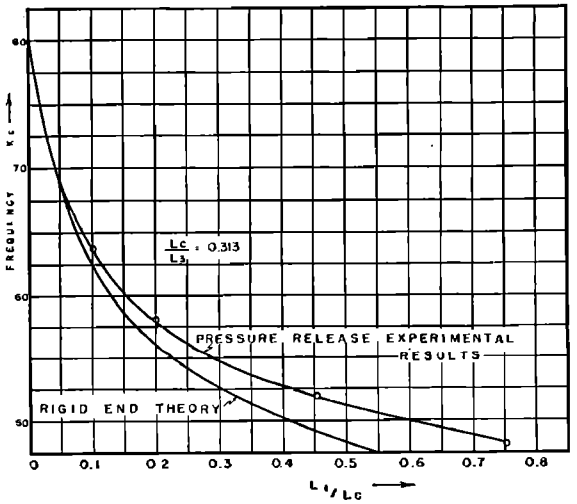

FIG. 20. Comparison of theoretical results for rigid end at $x=0$ with experimental values for pressure release at $x=0$.

results to be expected from a variable resonant frequency unit with all pressure release walls.

The graph of Fig. 20 is an indication of the difference between the theoretical values for the resonant frequency as a function of the ratio L_1/L_c, obtained on the basis of a rigid end calculation for cross-section dimensions of the liquid backing four times the crystal cross-section dimensions and the experimental results for a pressure release end. As can be seen from the graph for short lengths of backing liquid, the agreement is close. Even for the longer lengths, the rigid end theory indicates the general direction of the experimental results.

It has been indicated in Sec. II-C on volume losses that such losses can be neglected in discussing the operation of the present experimental units; support losses considered in Sec. II-D would be expected to decrease as the frequency of the unit decreased, since the region of support would more nearly coincide with a node at the lower frequencies. Losses in the material used to bond the coupling plate to the crystal are not the predominating source of loss, as shown by a direct experimental test. It appears, therefore, that the interface losses between the mercury and the supporting container are predominant in the present experimental units. This would yield the type of relation between the quality factor and the frequency obtained experimentally (see Fig. 14).

V. ACKNOWLEDGMENT

We wish to thank Mr. Frank J. Fry for contributions to this investigation. Mr. L. L. Howard was in charge of the IBM calculations for this work. Mr. H. D. Frankel and Mr. N. C. Marsh also contributed to the extensive numerical computations.

NOTATION

Roman Symbols

$a_{1\lambda}=L_1/\lambda$.

A_c = cross-sectional area of the crystal.

A_{nm} : coefficient determined by boundary conditions at $x=0$.

$b_{13}=L_1/L_3$.

b_l, b_{kl} : defined by (24).

$c_{32}=L_3/L_2$.

$C=-j\omega\rho C'$.

C' : x component of the particle velocity (time free) looking into the backing at $x=0$.

d_r : defined by Eq. (24).

$E_{nm}=[4a_{1\lambda}^2-b_{13}^2(n^2+m^2c_{32}^2)]^{\frac{1}{2}}$.

E_b : energy loss per second in the bonding material.

E_s : energy loss per second at the support for the crystal unit.

F : force exerted on the backing at $x=0$.

$G=(\pi^4/2^7)(Z_a/j\rho V)$; $G'=(\pi^2/2^4)(Z_a/j\rho V)$.

G_{nm} : defined by expression (14).

$H_{nm}=h_l$: defined by expression (13); $h_l'=h_l/C'$.

$k=\omega/V$.

$K=V_c/L_c$.

L_1, L_2, L_3 : dimensions of the backing along the x, y, and z directions. L_1 is the continuously variable dimension.

L_c : length of the crystal, L_p perimeter of crystal at support.

p, P : acoustic pressure distribution functions ($p=Pe^{j\omega t}$).

$P_{nm}=P_l$: pressure distribution function for the n, m mode.

$q_l=\sin(n\pi z/L_3)\sin(m\pi y/L_2)$.

Q' : quality factor, ratio of antiresonant impedance to resonant impedance.

r, s : one-half the crystal unit cross-section dimensions.

R_{aw} : input acoustic resistance into the walls of the container which support the liquid backing.

R_m : resistive component of the mechanical impedance on the crystal.

R_{mb} : resistive component of the mechanical impedance into the backing liquid at the coupling material-backing liquid interface. $R_{mb}\sim R_m$ if the interface losses predominate.

u_x, u_y, u_z, u_n : particle velocity components along the x, y, and z directions; n designates any one.

$u_{xnm}=u_{xl}$: x component of the particle velocity associated with the n, m mode.

U_n' : normal particle velocity amplitude at the wall, positive direction into the wall.

V, V_c : sound velocity (subscript c refers to crystal).

x, y, z : position coordinates.

Z_a : average input acoustic impedance into the backing.

Z_m : mechanical impedance.

Greek Symbols

α_{rk} : defined by expression (28).

$\beta_{nm}=\beta_i$: defined by expression (15).

γ_c, γ_r, $\gamma_{ar}=\omega L_c/V_c$: subscript c refers to crystal; r and ar denote resonance and antiresonance, respectively.

$\theta=\varphi^2/Z_0KC_0\gamma_0$.

λ, λ_c : wavelength of sound (subscript c refers to crystal).

ρ, ρ_c : density (subscript c refers to crystal).

$\varphi=(d/s)l_w$ for longitudinal mode;
$=(d/s)A_c/L_c$ for thickness mode.

d : piezoelectric constant, s : elastic constant.

l_w : width of electroded face, L_c : thickness of crystal.

A_c : area of electroded face (see for example, reference 5).

$\omega=2\pi f$, where f is the frequency.